Global Biogeochemical Cycles

RESEARCH ARTICLE
10.1029/2018GB006113

Dissolved Iron Supply from Asian Glaciers: Local Controls and a Regional Perspective

Xiangying Li[1,2,3], Yongjian Ding[2,4], Eran Hood[5], Robert Raiswell[6], Tianding Han[2], Xiaobo He[2], Shichang Kang[2,4], Qingbai Wu[3], Zhongbo Yu[1], Sillanpää Mika[7], Sha Liu[1], and Qijiang Li[8]

[1]College of Hydrology and Water Resources/State Key Laboratory of Hydrology-Water Resources and Hydraulic Engineering, Hohai University, Nanjing, China, [2]State Key Laboratory of Cryospheric Sciences, Northwest Institute of Eco-Environment and Resources, Chinese Academy of Sciences, Lanzhou, China, [3]State Key Laboratory of Frozen Soil Engineering, Northwest Institute of Eco-Environment and Resources, Chinese Academy of Sciences, Lanzhou, China, [4]University of Chinese Academy of Sciences, Beijing, China, [5]Environmental Science and Geography Program, University of Alaska Southeast, Juneau, AK, USA, [6]Cohen Biogeochemistry Laboratory, School of Earth and Environment, University of Leeds, Leeds, UK, [7]Laboratory of Green Chemistry, School of Engineering Science, Lappeenranta University of Technology, Mikkeli, Finland, [8]Hydrology and Water Resource Survey Bureau of Qinghai Province, Xining, China

Key Points:
- This study presents data of dFe from three glaciers in Asia over a full melt season and compiles a global dataset of dFe from over 12 glaciers
- Release of dFe from Asian glaciers is 23.7 Gg/a, and from global glaciers is 185 Gg/a, which is 4–10 times higher than from ice sheets
- Glaciers may provide a substantial but largely unrecognized source of potentially labile Fe and become increasingly important for global Fe cycle

Supporting Information:
- Supporting Information S1

Correspondence to:
Y. Ding and E. Hood,
dyj@lzb.ac.cn;
ewhood@alaska.edu

Citation:
Li, X., Ding, Y., Hood, E., Raiswell, R., Han, T., He, X., et al. (2019). Dissolved iron supply from Asian glaciers: Local controls and a regional perspective. *Global Biogeochemical Cycles*, *33*,1223–1237. https://doi.org/10.1029/2018GB006113

Received 22 OCT 2018
Accepted 25 AUG 2019
Accepted article online 28 AUG 2019
Published online 14 OCT 2019

Abstract Ice sheets have been shown to deliver large amounts of labile iron (Fe) to aquatic ecosystems; however, the role of glaciers distinct from ice sheets in supplying labile Fe to downstream ecosystems is less well understood despite their rapid volume loss globally. Direct and continuous measurements of Fe from glaciers throughout an entire melt season are very limited to date. Here we present extensive seasonal data on 0.45-μm-filtered Fe (dFe) from three glaciers in Asia. Concentrations of dFe are negatively correlated with glacier discharge, and dFe yields are closely related to specific discharge. Based on our study and previously published dFe data, we estimate the release of dFe from Asian glaciers to be 23.8±14.1 Gg/a. We further compile a global data set of dFe from more than 12 glaciers, which, when combined with data on glacier discharge, suggest that the release of dFe from glaciers globally is on the order of 185±172 Gg/a. This finding suggests that glaciers may provide a substantial, but largely unrecognized source of potentially labile Fe, and may become increasingly important for the Fe biogeochemical cycle in a warming climate.

1. Introduction

Quantifying the transport of riverine iron (Fe) is critical because it limits the primary productivity in downstream aquatic ecosystems, some of which receive substantial glacier discharge (Martin et al., 1990; Nielsdottir et al., 2009). Ice sheets have recently been shown to deliver large amounts of Fe to coastal ecosystems through outlet glaciers (Hawkings et al., 2014; Hodson et al., 2016, 2017) and icebergs (Raiswell, 2011; Raiswell et al., 2016, 2018). However, Fe release from glaciers distinct from Greenland and Antarctic ice sheets (Hood et al., 2015; Radić et al., 2014) remains poorly constrained at regional and global scales. There are differences in chemical weathering of Fe minerals between glaciers and ice sheets as a result of differences in water residence times, subglacial chemistry, and physical erosion rates (Bhatia et al., 2013; Brown et al., 1994; Schroth et al., 2011; Statham et al., 2008; Tranter et al., 1993). Discharge from glaciers exceeds that from ice sheets via outlet glaciers (Bamber et al., 2012; Bliss et al., 2014; Rignot et al., 2008), and climate modeling suggests that glacier discharge will be increasing at many regions (e.g., Arctic Canada, Svalbard, Russian Arctic) in coming decades (Intergovernmental Panel on Climate Change, 2013; Bliss et al., 2014; Dieng et al., 2017; Lutz et al., 2014). We contend that quantifying the release of Fe from glaciers is critical for understanding how glacier volume loss is impacting the transport of Fe from terrestrial to downstream aquatic ecosystems.

While a number of studies have been conducted on the concentration and/or export of Fe from ice sheets (Aciego et al., 2015; Bhatia et al., 2013; Hawkings et al., 2014; Hodson et al., 2017; Statham et al., 2008) and glaciers (Fortner et al., 2011; Galeczka et al., 2014; Li et al., 2013; Mitchell et al., 2001; Schroth et al., 2011; Zhang et al., 2015), there are no comprehensive regional or global estimates of the fluxes of Fe from glaciers. Previous studies indicated that dissolved Fe concentrations from some glaciers display a seasonal

variation and exhibit a positive correlation with glacier discharge (Hodson et al., 2016; Li et al., 2016; Mitchell et al., 2001). However, measurements of temporal variations in Fe across an entire glacier melt season are very limited. This paucity of data can be attributed to the challenging logistics of sampling glacial outflow in remote glacial basins. Having a comprehensive seasonal time series of Fe is critical given that solute concentrations can have strong seasonality as a result of the evolution of subglacial drainage system and chemical weathering therein (Hodson et al., 2010, 2016; Mitchell et al., 2001).

Glacially derived Fe has been distinguished in three forms: truly dissolved Fe (pore size < 0.02 μm), colloidal/nanoparticulate Fe (0.02 to 0.45 μm), and sediment-bound nanoparticulate Fe (>0.45 μm; Statham et al., 2008; Raiswell & Canfield, 2012; Hawkings et al., 2014). Recent studies in the Greenland and Antarctica showed that the largest source of Fe is sediment-bound Fe, while truly dissolved Fe is typically the least abundant phase (Hawkings et al., 2014; Hodson et al., 2017; Raiswell et al., 2018; Statham et al., 2008). Here we present a comprehensive data set of the concentrations and fluxes of filtered Fe (dFe; <0.45 μm) from three Asian glaciers over an entire melt season (Supporting Information S1). These data, combined with previously published data, provide a comprehensive estimate of the release of dFe from glaciers in Asia (ASG). We further use previously published data to estimate dFe fluxes from glaciers in other five regions including: Alaska (ALG), Central Europe (CEG), Svalbard and Jan Mayen (SJG), Low Latitudes (LLG), and Iceland (ICG). We propose that the release of dFe associated with glaciers globally may become increasingly important for the Fe biogeochemical cycle in a warming climate. Here we present a comprehensive data set of the concentrations and fluxes of filtered Fe (dFe; <0.45 μm) from threeAsian glaciers over an entire melt season (Supporting Information S1).

2. Materials and Methods

2.1. Site Description

Dongkemadi Glacier (DG, 16.4 km^2) and Laohugou Glacier (LHG, 20.4 km^2) in the Tibetan Plateau and Urumqi Glacier No.1 (UG1, 1.65 km^2) in the Tianshan Mountains range in altitude from 5,275 to 6,049 m, 4,260 to 5,481 m, and 3,740 to 4,486 m above sea level (asl), respectively (Figure 1). Overall, the regional climate is controlled by westerlies and southwest monsoon and is featured by warm-wet and cold-dry seasons. DG, UG1, and LHG are roughly representative of glacial drainage systems and Fe minerals for many glaciers in Asia, such as Koxkar Glacier (KOG, 82.9 km^2; Wang et al., 2010), Qiyi Glacier (QG, 2.87 km^2; Li et al., 2013), and Rongbuk Glacier (RBG, 152 km^2; Liu et al., 2000; Figure 1). Within China, glaciers (<20 km^2) make up 99% of glacier population, 49% of glacier volume and 74% of glacier area, and 98% of these glaciers occur within 3,000 to 6,500 m asl (Liu et al., 2015). Thus, DG, UG1, LHG, and QG are broadly representative of total population of Asian glaciers (Liu et al., 2015; Li et al., 2018, 2019; Pfeffer et al., 2014; Radić et al., 2014).

2.2. Sample Collection

Sampling was conducted at DG, UG1, and LHG over a full melt season in 2013 and 2017 (Figure 1 and Table 1). At DG, meltwater runoff was sampled bihourly at S1 (with a drainage area of 28.0 km^2) between May and September and at S2 (38.3 km^2) and S3 (52.8 km^2) during four diurnal cycles D1 (7–8 June), D2 (5–6 July), D3 (5–6 August), and D4 (22–23 September) in 2013. S1, S2, and S3 are located 0.5, 4.8, and 9.8 km from glacier terminus respectively. At UG1, the runoff was sampled twice daily (9:00 and 17:00) between May to September and bihourly during four diurnal cycles D1 (2–3 June), D2 (5–6 July), D3 (9–10 August), and D4 (31 August to 1 September) at site S (3.34 km^2) 0.3 km from glacier terminus in 2013. At LHG, the runoff was sampled once daily at site S (32.0 km^2) 1 km from glacier terminus between June to September in 2017. After sampling, samples were immediately filtered through 0.45-μm WCN membranes in a designated lab tent or room. Some filtrate was acidified with Optima HNO_3^- to pH<2 for dFe and Li analysis, while other filtrate was unacidified for ion analysis. Blank samples were taken using Milli-Q water by the same procedure. Samples were transported to the SKLCS at the CAS and kept frozen until analysis (Li et al., 2016). Sampling equipment was sequentially soaked in a 6 M HCl acid bath (48 hr), washed 20 times with 18.2 MΩ/cm Milli-Q water, soaked in a 6 M HNO_3 acid bath (48 hr), and washed 20 times with Milli-Q water before drying in a laminar flow hood. All sampling bottles were trace metal grade Nalgene low-density polyethylene.

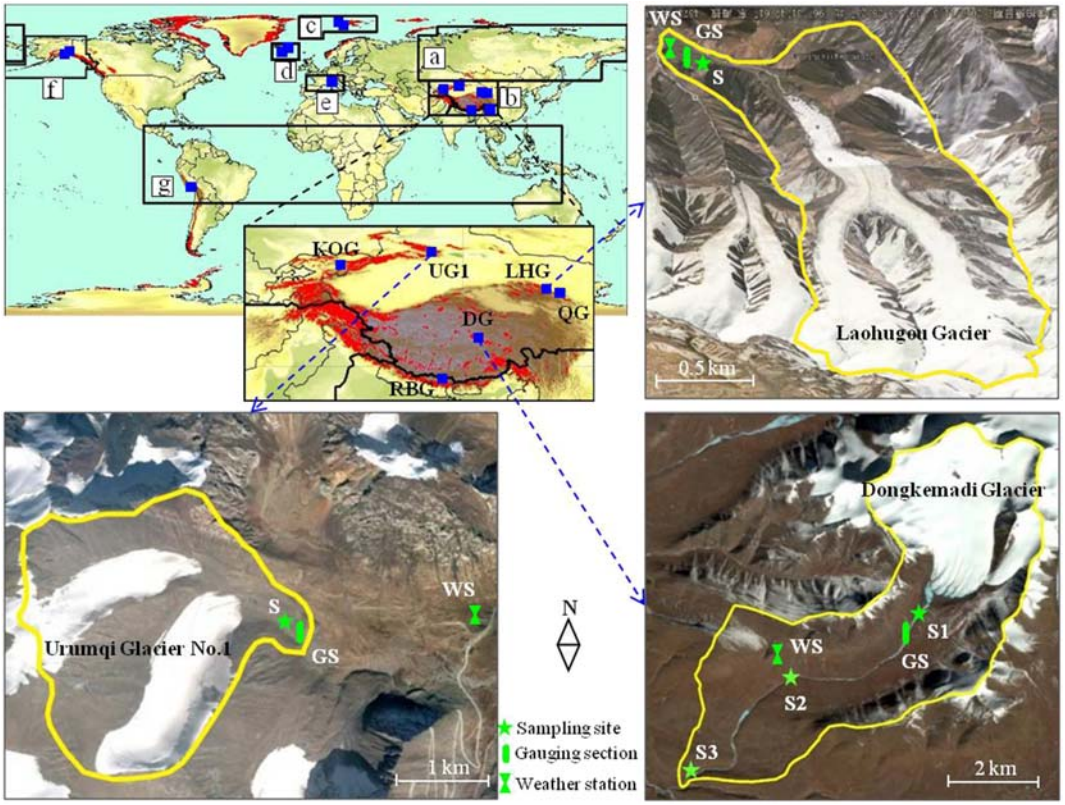

Figure 1. Location of Urumqi Glacier No.1 (UG1), Dongkemadi Glacier (DG), and Laohugou Glacier (LHG) as well as Qiyi Glacier (QG), Koxkar Glacier (KOG), and Rongbuk Glacier (RBG) in Asia. Sampling sites (S, S1, S2, and S3), weather stations (WS), and gauging sections (GS) are marked at UG1, DG, and LHG. Glaciers are shown in red, and the outflow sampling sites (blue squares) are widely distributed in (a and b) Asia, (c) Svalbard and Jan Mayen, (d) Iceland, (e) Central Europe, (f) Alaska, and (g) Low Latitudes. Note that glaciers in North Asia (a) only accounts for 5% of glacier population and 3% of glacial areas in the whole of Asia (a and b), which however is dominated by glaciers in the central and south Asia (b) (Pfeffer et al., 2014).

2.3. Laboratory Analysis

Four samples daily (4:00, 10:00, 16:00, and 22:00 hr) were analyzed at S1 (DG), and all samples were analyzed at S2, S3 (DG), and S (UG1 and LHG). Concentrations of dFe and Li were determined by inductively coupled plasma mass spectrometry (X-7 Thermo Elemental) at the Key Laboratory of Tibetan Environment Changes and Land Surface Processes at the CAS. The external calibration was used, and indium was added into samples as an internal standard. The analytical standard was measured after initial calibration, and then once every five samples. Detection limits were 24.3 nM for dFe and 4.3 nM for Li. Accuracy of analytical protocol was determined by repeated measurements of reference solution. Relative standard deviations of element concentrations in reference material were <5%. Cations and anions were determined by Dionex-600 and Dionex-2500 ICS, respectively. Detection limit was <435 nM, and precision was ±1%. HCO_3^- was determined by ion charge balance with the errors <5%. In blank samples, concentrations of dFe, Li, and ions were lower than detection limits, suggesting negligible contamination during sampling, transportation, and storage. Detailed methods can be found in Li et al. (2013, 2016, 2019).

2.4. Water and dFe Flux Estimates

Water fluxes from DG, UG1, and LHG were calculated by measuring discharge at gauging sections below 1 km from glacier terminus (Figure 1). The detailed method can be found in Li et al. (2018). Annual discharge data are summarized in Table 1. For glacier discharge from six glacial regions (ASG, ALG, CEG, SJG, LLG, and ICG), we used the annual average discharge (defined as all melt and rain water that runs off the glacierized area without refreezing) during 2003 to 2022, which is derived from the glacier mass balance model and

Global Biogeochemical Cycles

10.1029/2018GB006113

Table 1

Summary Statistics for Basin Bedrock, Glacier Areas and Discharges, Distances of Sampling Sites From Glacier Terminus, Sampling Periods, Pore Sizes of Membranes, and Mean Concentrations (±SE) and Ranges of Filtered Fe (dFe) in Proglacial Rivers Draining Four Glaciers (Urumqi Glacier No.1, Laohugou Glacier, Dongkemadi Glacier, and Qiyi Glacier) in Asia (ASG), As Well As Draining More Than Two Glaciers in Alaska (ALG), One Glacier in Central Europe (CEG), Two Glaciers in Svalbard and Jan Mayen (SJG), One Glacier at Low Latitudes (LLG), and Two Glaciers in Iceland (ICG)

Glacier	Bedrock	Glacial area (km^2)	Glacier discharge (10^6 m^3/a)	Distance from glacier terminus (km)	Sampling period	Pore size (μm)	Mean (nM)	Range	Sample size	Source
Dongkemadi Glacier (ASG)	Carbonate-rich	16.4	27.3	0.5	29 May to 30 September 2013	0.45	942 (522)	373–3,445	495	This study
Urumqi Glacier No.1 (ASG)	Carbonate-rich	1.65	2.94	0.3	31 May to 30 September 2013	0.45	818 (302)	222–1,891	162	This study
Laohugou Glacier (ASG)	Carbonate-rich	20.4	28.4	<1	3 June to 15 September 2017	0.45	1,559 (916)	265–4,298	40	This study
Qiyi Glacier (ASG)	Carbonate-rich	2.87	3.81[a]	0.5	August 2010	0.45	394 (719)[b]	8–1,747	12	Li et al. (2013)
Childs Glacier (ALG)	N/A	N/A	N/A	Adjacent	August 2008	0.45	109 (N/A)[c]	N/A	1	Lippiatt et al. (2010)
Unnamed Glaciers (ALG)	N/A	N/A	N/A	N/A	August 2008 and October 2009	0.45	7,403 (4,186)[d]	3,015–15,427 [d]	13	Schroth et al. (2011)
Haut Glacier d'Arolla (CEG)	Igneous/metamorphic	6.3	15.4	Adjacent	June to August 1999	0.45	6,964 (N/A)	268–21,429	132	Mitchell et al. (2001)
Austre/Vestre Brøggerbreen (SJG)	Sedimentary/mixed	16	30.0	0.5	August 2012/2013	0.40	568 (N/A)[e]	401–734[e]	2	Zhang et al. (2015)
Bogerbreen (SJG)	Sedimentary/mixed	3.3	N/A	1	June to August 2012	0.45	451 (208)[f]	212–821[f]	7	Hodson et al. (2016)
Rio Quilcay (LLG)	N/A	N/A	N/A	<5	July 2008	0.45	8,766 (7,843)[g]	1,786–21,429[g]	11	Fortner et al. (2011)
Vatnajökull Glacier (ICG)	Igneous-rich	8,100	N/A	<10	July 2011	0.20	780 (584)[h]	160–1,450[h]	5	Galeczka et al. (2014)
Kötlujökull Glacier (ICG)	Igneous-rich	600	N/A	<5	July 2011	0.20	143 (70)[i]	70–210[i]	3	Galeczka et al. (2014)

Note. N/A denotes no available data.
[a]Value from Song et al. (2008). [b]Value that is corrected by the ratio (0.63) of monthly (August) to seasonal mean concentration from adjacent Laohugou Glacier (LHG) over a full melt season in 2017. [c]Value from sample G1 from glacial melt draining Childs Glacier. [d]Values from the sum of soluble Fe (<0.02 μm) and colloidal Fe (0.02–0.45 μm). [e]Values from samples at HBR that is close to Austre Brøggerbreen Glacier. [f]Values from samples at EU that is close to Bogerbreen Glacier. [g]Values from samples at sites 1 to 10 and 12 that are close to Cuchilla Cocha Glacier and Andavite 5518 Glacier. Note that the abnormal values (>5 mg/L) are excluded. [h]Values from samples at Hágöngulón and Sveðja that are close to Vatnajökull Glacier. [i]Values from samples at the west bank of Múlakvísl, background sample, and ice block that are close to Kötlujökull Glacier.

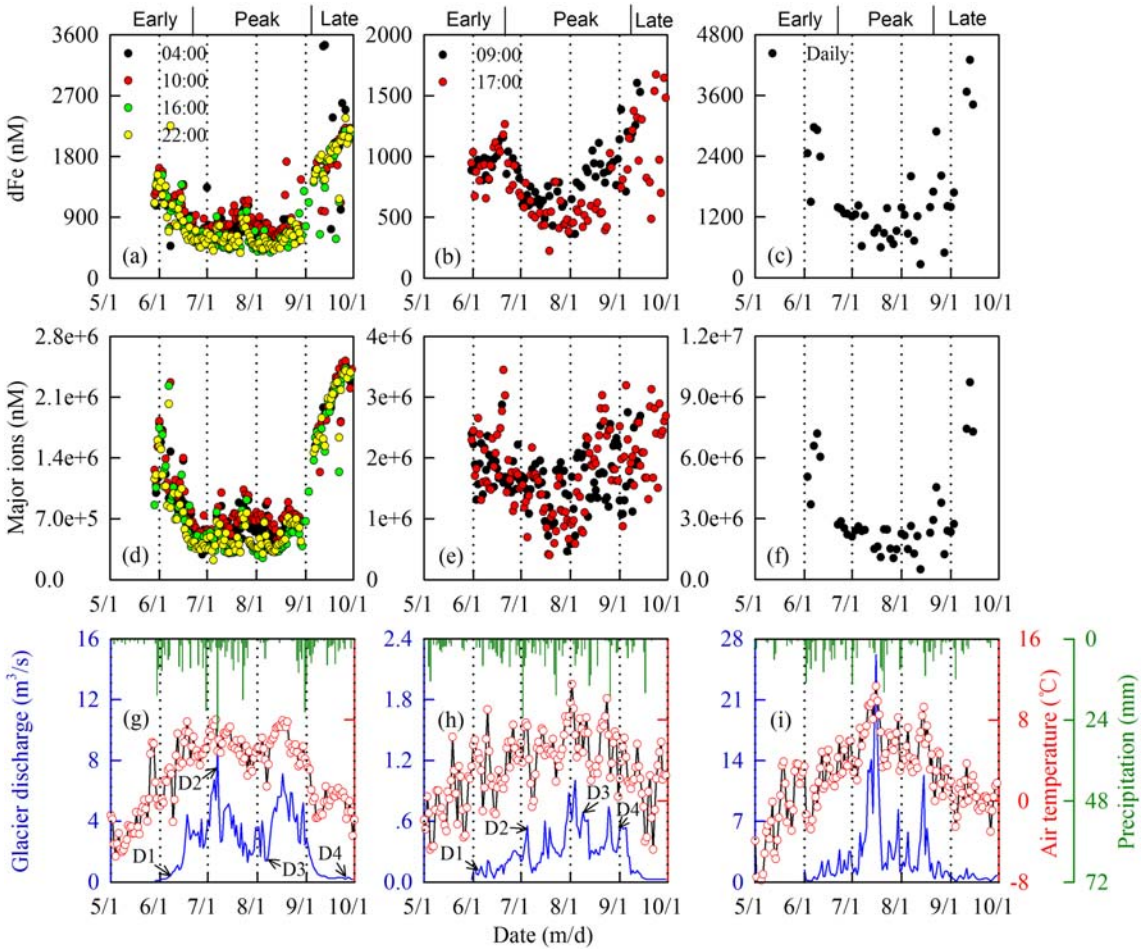

Figure 2. Daily hydrology, climate, and hydrochemistry from Dongkemadi Glacier (DG; a, d, and g), Urumqi Glacier No.1 (UG1; b, e, and h), and Laohugou Glacier (LHG; c, f, and i) proglacial rivers for DG (at S1), UG1, and LHG (at S): (a–c) filtered Fe (dFe) concentrations, (d–f) summed major ion (Na^+, K^+, Ca^{2+}, Mg^{2+}, Cl^-, NO_3^-, SO_4^{2-}, and HCO_3^-) concentrations, and (g–i) glacier discharge, air temperature, and precipitation at seasonal timescales during May to September. Note that Early, Peak, and Late denote the early melt, peak flow, and late melt seasons, respectively.

global climate models (Bliss et al., 2014). Here, glacier discharge from these six glacial regions was estimated as 359×10^9 m^3/a for ASG, 338×10^9 m^3/a for ALG, 73×10^9 m^3/a for SJG, 51×10^9 m^3/a for ICG, 15×10^9 m^3/a for LLG, and 9×10^9 m^3/a for CEG. dFe fluxes from DG, UG1, and LHG were calculated by daily dFe concentrations multiplied by discharge. During absent sampling days for LHG, dFe concentrations were estimated by the best fit regression between measured discharge (m^3/s) and dFe concentration (nM; $y=1{,}545x^{-0.339}$, $R^2=0.34$, $p<0.01$). To calculate dFe flux from ASG, we use annual mean discharge multiplied by seasonal mean dFe concentration from DG, UG1, LHG, and QG (Table 1). This approach was used to calculate dFe fluxes from ALG (based on dFe data from Childs Glacier and Unnamed Glaciers), CEG (Haut Glacier d'Arolla), SJG (Austre/Vestre Brøggerbreen and Bogerbreen), LLG (Rio Quilcay in Peru), and ICG (Vatnajökull Glacier and Kötlujökull Glacier; Table 1). Error estimates for dFe fluxes were calculated as standard deviations of dFe concentrations multiplied by discharge.

3. Results

Concentrations of dFe from DG (at S1), UG1, and LHG (at S) spanned more than an order of magnitude (222 to 4,298 nM; Table 1). Concentrations of dFe and major ions displayed strong seasonality, with higher values during May–June and September (low-flow seasons) and lower values during July–August (high-flow seasons; Figures 2a–2c). At diurnal timescales, dFe concentrations from DG (at S1, S2, and S3) and UG1 exhibited a complex variation. During low-flow seasons on either side of melt season (D1 and D4), dFe

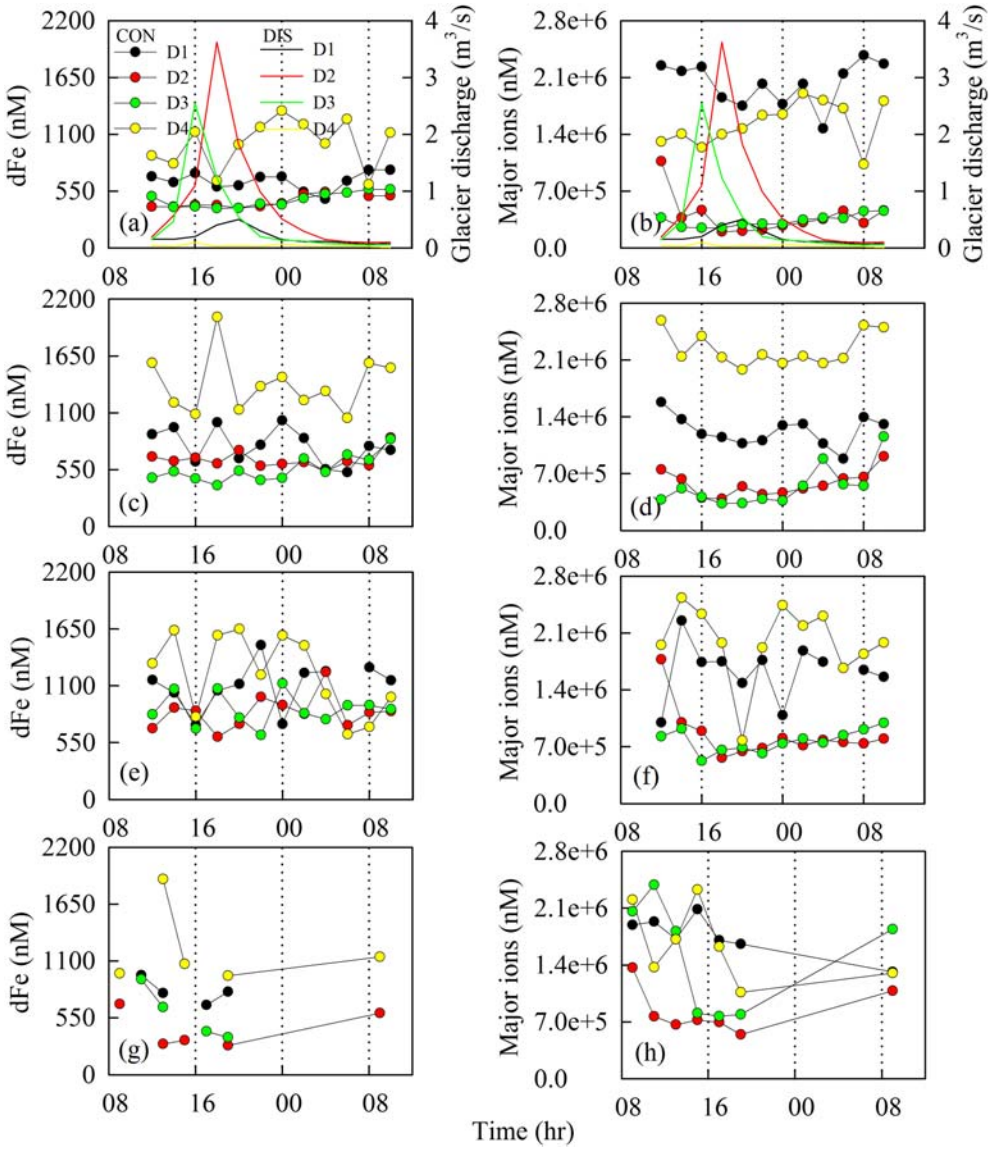

Figure 3. Bihourly filtered Fe (dFe) and summed ion concentrations (CON) and/or glacier discharge (DIS) from proglacial rivers draining Dongkemadi Glacier (DG) at sites (a and b) S1, (c and d) S2, and (e and f) S3, and draining Urumqi Glacier No.1 (UG1) at site (g and h) S at diurnal timescales (D1, D2, D3, and D4; Figure 2) during June to September.

concentrations were variable and showed unconspicuous diurnal trend (Figures 3a, 3c, 3e, and 3g). During the melt season (D2 and D3), higher values usually occurred in the morning hours (2:00–10:00 hr) with lower values in the afternoon and evening hours (16:00–0:00 hr) at S1 and S2 for DG and at S for UG1 (Figures 3a, 3c, and 3g). At S3, daily variations in dFe concentrations are not obvious (Figure 3e). Changes in the concentration of major ions from DG, UG1, and LHG followed a similar seasonal pattern to dFe concentrations and exhibited a clear inverse relationship to glacier discharge at diurnal and seasonal timescales (Figures 2 and 3).

Fluxes of dFe from DG (at S1), UG1, and LHG (at S) exhibited strong seasonality, with higher values during peak flow seasons and lower values during the early and late melt seasons. Although dFe concentrations were higher during the early and late melt seasons, these fluxes only accounted for 17%, 14%, and 30% of total dFe fluxes from DG, UG1, and LHG, respectively (Figure 4). Daily dFe fluxes from DG, UG1, and LHG were positively related to glacier discharge, and the cumulative discharge and fluxes increased sharply during peak discharge from early July through to August for DG, from late July to early September for UG1, and

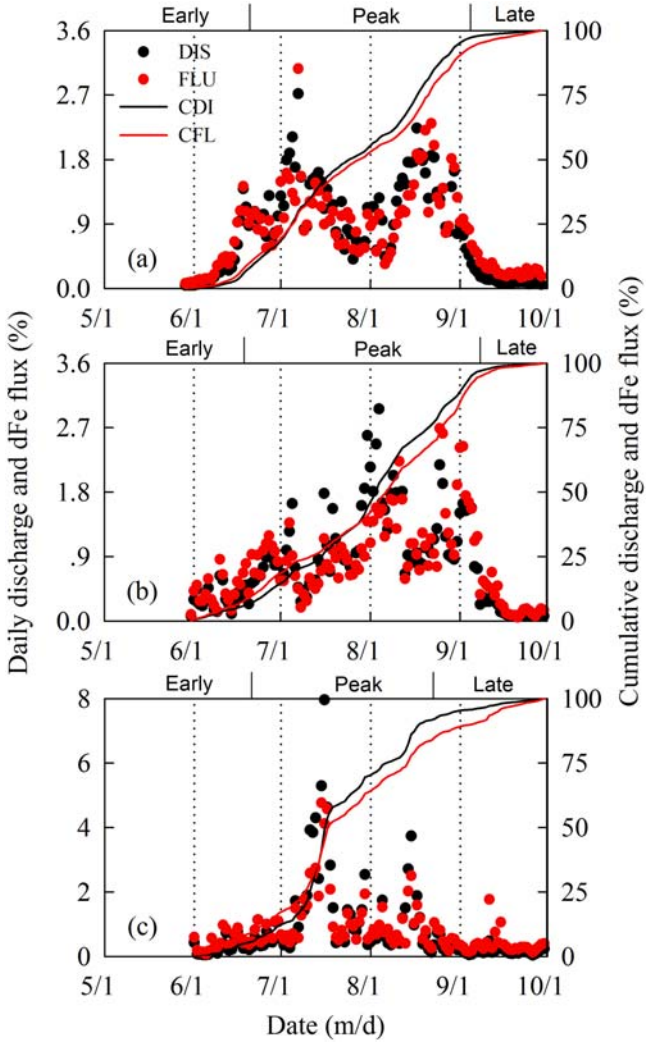

Figure 4. Daily (DIS) and cumulative (CDI) glacier discharges (percentages), as well as daily (FLU) and cumulative (CFL) filtered Fe (dFe) fluxes from (a) Dongkemadi Glacier (DG; at S1), (b) Urumqi Glacier No.1 (UG1), and (c) Laohugou Glacier (LHG) at seasonal timescales during May to September. Note that Early, Peak, and Late denote the early melt, peak flow, and late melt seasons, respectively.

from early July to middle August for LHG. The largest daily flux occurred in July for DG (33.9 kg/day), in August for UG1 (3.15 kg/day), and in July for LHG (74.9 kg/day), and the smallest daily flux was in May for DG (0.44 kg/day), in September for UG1 (0.06 kg/day), and in June for LHG (1.04 kg/day; Figure 4). Total glacier discharges per year were 27.3×10^6 m^3 for DG, 2.94×10^6 m^3 for UG1 in 2013, and 28.4×10^6 m^3 for LHG in 2017, which transported an estimated 1,105±798 kg Fe from DG, 117±50 kg Fe from UG1, and 1,572±1,457 kg Fe from LHG (Table 2). This equated to melt season area-weighted dFe yields (dFe flux divided by the contributing drainage area) of 39.5±28.5 kg · km^{-2} · a^{-1} for DG, 35.0±15.0 kg · km^{-2} · a^{-1} for UG1, and 49.1±45.5 kg · km^{-2} · a^{-1} for LHG (Table 2).

The range of dFe concentrations from DG (at S1), UG1, and LHG (at S) overlap those in the majority of previously published data from glaciers globally (Table 1). Here, we scaled up our data from DG, UG1, and LHG, in combination with published data from QG in Asia, to estimate a regional dFe flux as 23.8±14.1 Gg/a from ASG (Table 3). Similarly, regional dFe glacial fluxes were estimated at 71.1±79.2 Gg/a from ALG, 7.4±6.6 Gg/a from LLG, 3.5 Gg/a from CEG, 2.1±0.9 Gg/a from SJG, and 1.3±0.9 Gg/a from ICG. This equated to glacier area-weighted dFe yields of 3,139 ±2,808 kg · km^{-2} · a^{-1} for LLG, 1,701 kg · km^{-2} · a^{-1} for CEG, 820±914 kg · km^{-2} · a^{-1} for ALG, 195±116 kg · km^{-2} · a^{-1} for ASG, 61±25 kg · km^{-2} · a^{-1} for SJG, and 119±84 kg · km^{-2} · a^{-1} for ICG (Table 3). The yields were derived from dFe flux divided by glacial area as the drainage area data were not available in all cases. Some regions are poorly represented with estimates based on a single glacier and/or on a relatively small sample size (SJG, LLG, and ICG). However, the fluxes and yields from these regions are relatively low, and overall our data permits some cautious conclusions to be drawn.

4. Discussion

4.1. dFe Concentrations and Discharge

Changes in discharge reflect not only the diurnal and seasonal variations in glacier ablation and water generation but also the balance of melting, refreezing, and water storage changes at glacial basins (Hodgkins, 2001; Hodgkins et al., 2013). Glacier discharge is closely related to climate, with higher discharge occurring as a result of increases in air temperature and/or precipitation (Figures 2g–2i). Previous studies have showed that solutes in glacier runoff are primarily derived from bedrock weathering (>71%) and less from atmospheric deposition (<4%) and sea-salt deposition (<25%; e.g., Hodgkins et al., 1997; Hodson et al., 2000, 2002; Sharp et al., 1995; Yde et al., 2005, 2008). Therefore, seasonal variations in the concentration of dFe from DG, UG1, and LHG are largely reflective of the interactions between glacier meltwater and glacial sediments through the glacial runoff season (Li et al., 2016, 2019; Mitchell et al., 2001; Mitchell & Brown, 2007).

During glacier melt season, field observations showed that the subglacial drainage system evolves from a slow-inefficient drainage system (delayed flow) to a fast-efficient drainage system (fast flow) with well-developed drainage paths and then to a drainage system with channel configuration for DG, UG1, and LHG. Delayed flow transports meltwater primarily through ice-bedrock interface, which prolongs meltwater residence time in subglacial environments and encourages the acquisition of solutes (e.g., Hubbard et al., 1995; Hubbard & Nienow, 1997; Nienow et al., 1998). This leads to higher concentrations of dFe and major ions during the early (late May to mid-June) portions of the melt season (Figures 2a–2f). During the peak portion of the melt season (mid-June to late August), fast flow occurs mainly through ice-walled conduits and open channels, which reduces meltwater residence time and limits the potential for solute acquisition

Table 2
Specific Discharges, and Filtered Fe (dFe) Fluxes and Yields From Dongkemadi Glacier, Urumqi Glacier No.1, Laohugou Glacier, and Qiyi Glacier in Asia, As Well As From Haut Glacier d'Arolla in Central Europe (CEG) and Austre/Vestre Brøggerbreen in Svalbard and Jan Mayen (SJG)

Glacier	Specific discharge (m/a)	dFe flux (kg/a)	dFe yields ($kg \cdot km^{-2} \cdot a^{-1}$)	Sources
Dongkemadi Glacier	0.98	1,105±798	39.5±28.5	This study
Urumqi Glacier No.1	0.88	117±50	35.0±15.0	This study
Laohugou Glacier	0.89	1,572±1,457	49.1±45.5	This study
Qiyi Glacier	1.33	84±N/A	29±N/A	Li et al. (2013)
Haut Glacier d'Arolla	2.44	6,006±N/A[a]	953±N/A	Mitchell et al. (2001)
Austre/Vestre Brøggerbreen	1.88	954±N/A	60±N/A	Zhang et al. (2015)

Note. N/A denotes no available data.
[a]Value estimated by annual mean dFe concentration multiplied by annual discharge.

(e.g., Li et al., 2016, 2019; Mitchell et al., 2001; Wadham et al., 2001), thus resulting in lower concentrations of dFe and major ions (Figures 2a–2f). During late portion of the melt season (late August to late September), there is renewed storage of meltwater within the contracting englacial and/or subglacial conduits (Hodgkins, 2001; Hodgkins et al., 2013). This results in higher dFe and ion concentrations due to longer residence time of meltwater (Figures 2a–2f).

The seasonality of dFe concentrations at DG, UG1, and LHG is further reflected in the ratios of monthly to seasonal mean dFe concentrations, which range from 0.95 to 1.85 during the shoulder season months of June and September and from 0.63 to 0.92 during the peak runoff months of July and August. The seasonal amplitude of these ratios provides a template that can be used to estimate seasonal mean concentrations of dFe sampled during limited periods of glacier runoff season in other ASG glacial basins where the climate, bedrock, and weathering intensity are similar. For example, a mean seasonal dFe concentration at QG (394±719 nM) can be derived from limited August samples (mean=248±491 nM; n=12) by using the ratio of mean August to seasonal dFe concentrations (0.63) at nearby LHG (Table 1).

Over the whole melt season, the concentrations of dFe from DG, UG1, and LHG are significantly correlated with glacier discharge, with a power law relationship based on the best fit regression method (DG: $y=1{,}007x^{-0.310}$, $R^2=0.75$; UG1: $y=569x^{-0.196}$, $R^2=0.30$; LHG: see above), where y and x indicate daily

Table 3
Glacier Areas and Discharges, Mean Filtered Fe (dFe) Concentrations (Ranges), and dFe Fluxes and Yields (dFe Flux Divided by the Glacial Area) From Four Glaciers in Asia (ASG), More Than Two Glaciers in Alaska (ALG), One Glacier in Central Europe (CEG), Two Glaciers in Svalbard and Jan Mayen (SJG), One Glacier in Low Latitudes (LLG), and Two Glaciers in Iceland (ICG) During 2003–2022

Glacier	Glacial area (km^2)	Glacier discharge (10^9 m^3/a)	dFe concentration (nM)	dFe flux (Gg/a)	dFe yields ($kg \cdot km^{-2} \cdot a^{-1}$)	Sample size	Source
ASG	121,694[a]	359[b]	1,183±703[c] (8–4,298)[d]	23.8±14.1	195±116	709[d]	This study
ALG	86,715[a]	338[b]	3,756±4,186 (3,015–15,427)[e]	71.1±79.2	820±914	14[e]	This study
CEG	2,063[a]	9[b]	6,964±N/A (268–21,429)[f]	3.5±N/A	1,701±N/A	132[f]	This study
SJG	33,922[a]	73[b]	510±208 (212–821)[g]	2.1±0.9	61±25	9[g]	This study
LLG	2,346[a]	15[b]	8,766±7,843 (1,786–21,429)[h]	7.4±6.6	3,139±2,808	11[h]	This study
ICG	11,060[a]	51[b]	462±327 (70–1,450)[i]	1.3±0.9	119±84	8[i]	This study
Glaciers	726,792[a]	1,430[b]	2,408±3,246 (8–21,429)[j]	185±172	254±237	883[j]	This study
Greenland ice sheet	1,711,279[k]	418–665	706±659 (232–4,701)	16.5–26.3	9.6–15.4[l]	66	Hawkings et al. (2014);
Antarctic ice sheet	12,295,000[m]	33–254	653±386 (82–1,343)	3.0–25.8	0.2–2.1[l]	79	Green et al. (2005); Hawkings et al. (2014); Hodson et al. (2017)

Note. These data are combined to produce the global estimates of the fluxes and yields of dFe from glaciers globally. N/A denotes no available data.
[a]Value from Pfeffer et al. (2014). [b]Value from Bliss et al. (2014). [c]Value denotes discharge-weighted mean dFe concentration. [d]Value that is calculated based on data from this study and Li et al. (2013). [e]Value that is calculated based on data from Lippiatt et al. (2010) and Schroth et al. (2011). [f]Value from Mitchell et al. (2001). [g]Value that is calculated based on data from Zhang et al. (2015) and Hodson et al. (2016). [h]Value from Fortner et al. (2011). [i]Value that is calculated based on data from Galeczka et al. (2014). [j]Value that is calculated based on data from this study, as well as Mitchell et al. (2001), Lippiatt et al. (2010), Schroth et al. (2011), Fortner et al. (2011), Li et al. (2013), Galeczka et al. (2014), Zhang et al. (2015), and Hodson et al. (2016; Table 1). [k]Value from Kargel et al. (2012) and Pfeffer et al. (2014). [l]Value that is calculated based on dFe flux divided by ice sheet area. [m]Value from Fretwell et al. (2013).

mean dFe concentration (nM) and discharge (m^3/s), respectively. This exponential relationship can be attributed to the nonlinear processes of coupled meltwater production, solute acquisition, and meltwater dilution and supports a strong hydrological control on the concentrations of dFe. This finding has important implications for efforts to calculate the seasonal dFe concentration and the export of dFe from glaciers (adjacent to DG, UG1, and LHG) where only measured or modeled glacier discharge is available.

Our discharge-weighted mean concentration of dFe from DG, UG1, and LHG is 1,183±703 nM (n=697), which is within the range of mean concentrations of dFe from other glaciers (109–8,766 nM; Table 1). The range of concentrations of dFe (222–4,298 nM) also overlaps those in the majority of published studies for glaciers (Table 1) and ice sheets (20–9,310 nM; Aciego et al., 2015; Bhatia et al., 2013; Galeczka et al., 2014; Green et al., 2005; Hawkings et al., 2014; Hodson et al., 2017; Statham et al., 2008; Yde et al., 2014). Published concentrations of dFe reported for glaciers range from 8 to 21,429 nM, with a mean concentration of 2,842±3,687 nM (n=186; Table 1). This mean value is almost quadruple than estimated for global rivers (720 nM; De Baar & de Jong, 2001). Overall, the concentrations of dFe from glaciers demonstrate high variability (Table 1), likely as a result of not only subglacial hydrology and bedrock and/or sediment composition but also climate, altitude, sampling regime (e.g., frequency and seasonality of samples), and the distance of sampling sites from the glacier terminus.

Temporal variations in the flux of dFe from DG, UG1, and LHG can largely be attributed to glacier discharge, which changed on daily and seasonal timescales. This is consistent with previous studies that showed that dFe fluxes are dominated by glacier discharge rather than dFe concentration (Li et al., 2016; Mitchell & Brown, 2007). For example, at Haut Glacier d'Arolla in Switzerland, dFe concentrations exhibit a similar seasonal pattern with export increasing with glacier discharge (Mitchell et al., 2001). Thus, the majority of glacially derived dFe is released during peak glacier melt season. Although dFe fluxes from DG and LHG are 9.4 and 11.3 times higher than that from UG1, the yields from UG1 are comparable with those from DG and LHG, which drain larger areas and have higher discharge (Table 2). Namely, in regions where glaciers have similar dFe concentrations, dFe yields are largely controlled by specific discharge. For example, Haut Glacier d'Arolla basin with high specific discharge and elevated concentrations of dFe exhibits the largest dFe yields (Table 2).

4.2. Weathering and Transport Influences on dFe Concentration

Previous studies have shown that the dissolution of carbonate is the dominant weathering process in most glacial basins within China (Li, 2009) and that dFe at DG and QG results primarily from oxidation of pyrite (Li et al., 2013, 2016, 2019). The close relationships between dFe and SO_4^{2-}, Ca^{2+} (also Mg^{2+} and HCO_3^-; Figures 5a–5f) suggest that pyrite oxidation coupled to carbonate dissolution mainly governs dFe acquisition at DG, UG1, and LHG. Microbially mediated pyrite oxidation may also be coupled to the weathering of potassium and other silicate minerals (Nowak & Hodson, 2015). This is supported by the close relationships between dFe and Li (Figures 5g–5i) given that Kısakurek et al. (2005) showed that Li is predominantly derived from silicate weathering even in carbonate-dominated basins (Li et al., 2016, 2019). Hematite and/or siderite may also contribute dFe due to their wide distribution at DG and QG (Li et al., 2013, 2016). Aeolian dust that is rich in Fe similar to that deposited in snowpack at LHG (Dong et al., 2014) is another potential source of dFe.

Downstream, dFe increases from S1 to S2 and S3 (Figure 6). On average, seasonal mean dFe concentrations increase by 21% from S1 to S2 and by 61% from S1 to S3 over the whole glacier melt season. This downstream change is consistent with changes in dissolved organic carbon (DOC; Li et al., 2018) and is most likely related to snow melt and/or rain water leaching of Fe from sediment and/or soil minerals on surrounding mountain slopes (Li et al., 2016) or the release of dFe from melting permafrost (Han et al., 2016; Li et al., 2016). In contrast to our findings, dFe concentrations in the Bayelva River decreased 84% by ~4 km downstream from Austre Broggerbreen glacier (ABG) in Svalbard, which was attributed to removal processes associated with the aggregation and adsorption of nanoparticulate and colloidal Fe to particles (Zhang et al., 2015). This difference between DG and ABG may be related to well-developed soils and plants in proglacial area at DG (Li et al., 2018), in comparison to bare bedrocks and glacial deposits at ABG (Zhang et al., 2015). Noticeably, the hydrological process may affect downstream changes of Fe concentrations from glaciers (e.g., warm- and cold-based), and further studies should be conducted. Additionally, Quaternary sediments and Mesozoic clastics at DG are likely to be much more readily weathered than metamorphic rocks in Bayelva River

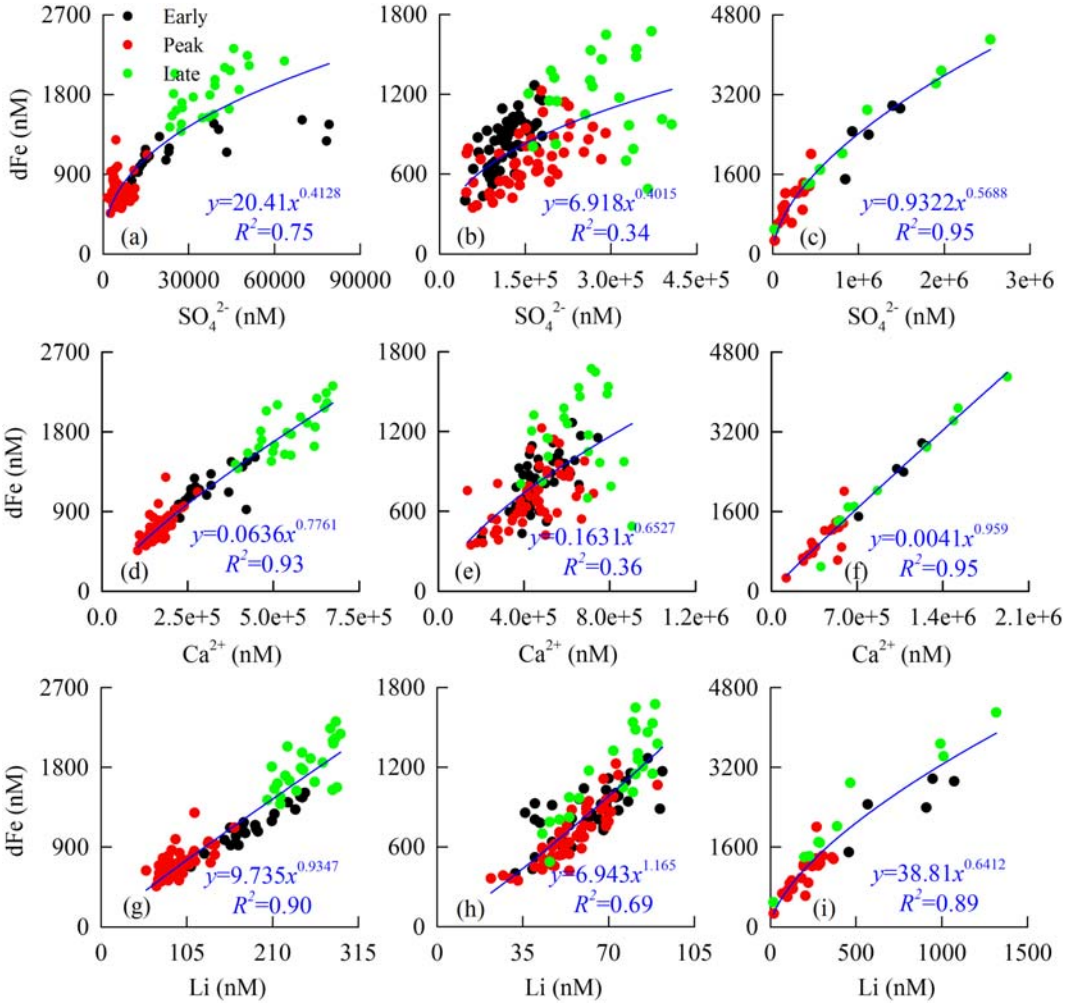

Figure 5. Relationships between daily filtered Fe (dFe) and (a–c) SO_4^{2-}, (d–f) Ca^{2+}, and (g-i) Li in proglacial rivers draining Dongkemadi Glacier (DG; at S1; a, d, and g), Urumqi Glacier No.1 (UG1; b, e, and h), and Laohugou Glacier (LHG; c, f, and i) over an entire melt season. The significant levels are below 0.001. Note that Early, Peak, and Late denote the early melt, peak flow, and late melt seasons, respectively.

basin (Li et al., 2016; Wu et al., 2009; Zhang et al., 2015). DOC concentrations may also play an important role in stabilizing dFe in meltwater runoff (Hodson et al., 2017), and it may be significant that the August DOC concentrations in the Bayelva river decrease away from the glacier (from 167 to 98 μM), whereas concentrations increase at DG downstream (51 to 74 μM over the same period (August); Li et al., 2018; Zhang et al., 2015). In any case, these findings highlight that the selection of sampling sites has important implications for studies of glacier meltwater hydrochemistry, which should be carried out as close as possible to the glacier terminus.

4.3. dFe Export and Implications

The elevated rates of chemical weathering beneath glaciers (Brown et al., 1994, 1996; Brown, 2002; Hood et al., 2015) indicate that glaciers may be a significant source of dFe. The global ecosystem-level significance of glacially derived dFe depends on both the mass of dFe and also on the behavior of dFe following its release to downstream ecosystems, which is outside the scope of this study. However, given that the glacial drainage systems, glacial erosion processes, access to comminuted sediment and subglacial sediment transfer are broadly similar at many glacial basins within Asia (e.g., Han et al., 2015; Li, 2009; Li et al., 2013, 2016, 2018, 2019; Wang et al., 2010), we use our data in combination with preexisting data to estimate a regional dFe flux from ASG as well as five other glacial regions across the globe (Table 3).

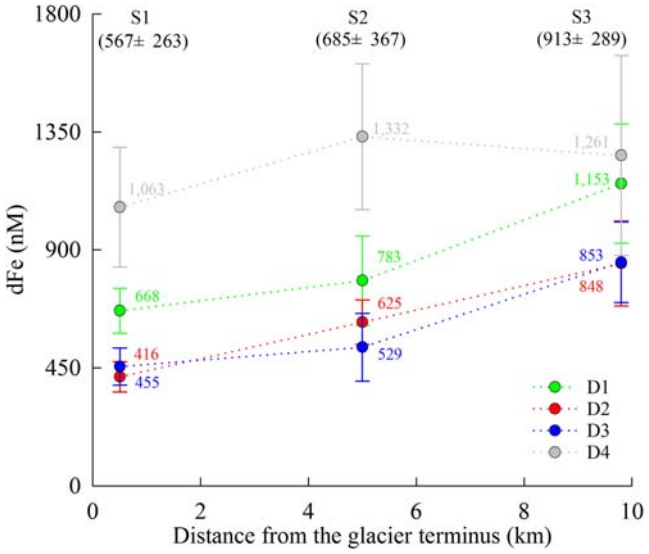

Figure 6. Variations in the concentration of filtered Fe (dFe) in proglacial rivers draining Dongkemadi Glacier (DG) at sites S1, S2, and S3 along the DG proglacial river during four diurnal cycles D1, D2, D3, and D4 over glacier melt season.

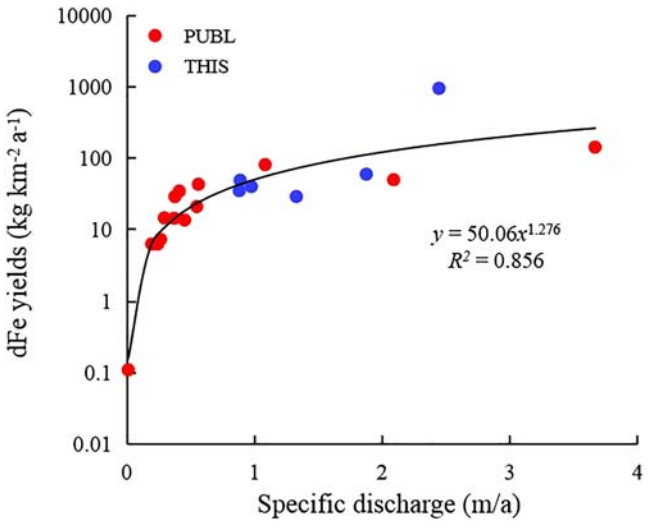

Figure 7. Annual specific discharge and filtered Fe (dFe) yields from glacial and ice sheet catchments. Note that PUBL denotes published data that was compiled in Yde et al. (2014), Hawkings et al. (2014), Lyons et al. (2015), and Hodson et al. (2016, 2017); THIS denotes data from Table 2 in this study; and HGA and AVB denote Haut Glacier d'Arolla and Austre/Vestre Brøggerbreen, respectively.

Notably, release of dFe from ASG only accounts for 21.8% of that from all six glacial regions despite its relatively large percentage (42.5%) of total glacier discharge. This indicates that using a single glacial region to represent any of the other five regions outside of ASG would introduce a large error into calculations of regional dFe release (see earlier). Yields of dFe are widely variable and decrease from LLG and CEG (>1,500 kg · km^{-2} · a^{-1}) to ALG (~800 kg · km^{-2} · a^{-1}) to ASG, ICG, and SJG (<200 kg · km^{-2} · a^{-1}). This trend is consistent with the power law dependence identified by Hodson et al. (2017) with higher yields resulting from higher specific discharge; however, some of the data sets we used are quite limited and further work is needed to support this inference. Based on limited data available, it appears that dFe yields from ASG, ALG, CEG, and LLG are larger than that from Greenland ice sheet (9.6–15.4 kg · km^{-2} · a^{-1}; Table 3). In general, the mean yields (1,006 kg · km^{-2} · a^{-1}) from six glacial regions (Table 3) are larger than that (217 kg · km^{-2} · a^{-1}, which is calculated by mean dFe concentration (2,336±443 nM), glacier discharge (149×10^9 m^3/a; Bliss et al., 2014) and glacial area (89,721 km^2; Pfeffer et al., 2014)) from 10 outlet glaciers draining Greenland ice sheet, including Leverett Glacier (mean dFe concentrations: 706±659 nM; Hawkings et al., 2014), Bristol Glacier (51±29 nM), and Bath Glacier (96±56 nM; Statham et al., 2008); Glacier "M" (3,790±210 nM), Glacier "O" (9,950 ±550 nM), and Glacier "N" (3,690±230 nM; Bhatia et al., 2013); and Qoorqup (4,060±2,447 nM), Russell/Isunnguata (505±137 nM), Kangaarsarsuup (230±92 nM), and Glacier "G" (286±19 nM; Aciego et al., 2015). This is consistent with generally higher specific discharge (1.97 m/a, which is based on glacier discharge (Pfeffer et al., 2014) divided by glacier area (Bliss et al., 2014) as the drainage area data were not available) and higher concentrations of dFe from glaciers (2,408 ±3,246 nM; Table 3) as compared to outlet glaciers (1.66 m/a and see above; Bliss et al., 2014; Pfeffer et al., 2014). The disproportionately high releases of dFe from ALG, CEG, and LLG relative to the size of their ice reservoirs reflect the high rates of glacier mass loss (Bliss et al., 2014; Meier et al., 2007; Intergovernmental Panel on Climate Change, 2013), as well as the high rates of physical bedrock weathering associated with glaciers in ALG, CEG, and LLG glacial regions in comparison to other three regions (ASG, SJG, and ICG; Table 3; Hallet et al., 1996).

Given that glacier discharge from these six glacial regions (845×10^9 m^3/a, which is comparable to the maximum estimate of the discharge from the Greenland and Antarctic ice sheets [919×10^9 m^3.a]; Table 3) accounts for 59.1% of total glacier discharge ($1,430\times10^9$ m^3/a; Bliss et al., 2014), we can crudely extrapolate global glacier dFe release at 185±172 Gg/a (Table 3). Thus, current release of dFe from glaciers quantitatively is 3.6–9.5 times higher than dFe release from ice sheets (19.5–52.1 Gg/a; Hawkings et al., 2014; Hodson et al., 2017). Although total discharge from glaciers is only 1.6 to 3.2 times higher than that from ice sheets (451–919 10^9 m^3/a; Hawkings et al., 2014; Hodson et al., 2017), its area-weighted dFe flux is 15 to 26 times higher than ice sheets (9.8–17.5 kg · km^{-2} · a^{-1}; Table 3).

Yields of dFe from maritime glaciers around Antarctica and Arctic (Hodson et al., 2017) show a nonlinear response to increasing specific discharge ($y = 48x^{1.23}$, where y and x indicate dFe yields and specific discharge, respectively). The yields we derived fit well with data of Hodson et al. (2017), and the resulting regression curve from the combined data ($y = 50x^{1.28}$, R^2=0.86, p<0.01) corresponds well with the Hodson curve (Figure 7). This combined regression equation indicates that dFe export per unit area increases by approximately 2 orders of magnitude when

glacier discharge is increased by an order of magnitude. This finding provides compelling evidence that glacial basins have a high potential for substantial dFe production and export to downstream ecosystems as glacier discharge increases in a warming climate.

The quantitative importance of dFe is consistent with DOC release from glaciers, which is far greater than the combined DOC export from ice sheets (Hood et al., 2015; Li et al., 2018). Although dFe release is considerable, its behavior in downstream ecosystems is difficult to constrain. Removal processes (see above) are related to many factors such as chemical flocculation, precipitation, and absorption (Hodson et al., 2016; Schroth et al., 2014; Zhang et al., 2015), but our data also show that downstream additions may occur in proglacial landscapes. These competing processes make it difficult to predict downstream behavior for dFe from ASG.

Our estimates contain substantial uncertainty. The largest source of uncertainty is the scarcity of data on the concentrations of dFe from glaciers. There is considerable regional variability in the concentration of dFe, and the data assembled here (Table 1) do not allow for any statistically valid inferences about how glacier size or discharge at basins with a similar bedrock influences the concentrations of dFe. For example, Haut Glacier d'Arolla (HGA) has a higher mean dFe concentration than UG1 and QG (which are substantially smaller than HGA; Mitchell et al., 2001; Li et al., 2013) and DG and LHG (which are larger than HGA; Table 1). This implies that our extrapolation from a small number of glaciers to produce the estimates of dFe flux have a high degree of uncertainty. Furthermore, field sampling only during high-flow seasons (June to August) may have resulted in low estimates of seasonal mean concentrations of dFe for most of glacial basins (Table 1). Moreover, samples filtered by smaller pore sizes (0.2 or 0.4 μm) may also generate lower concentrations of dFe than filtered by 0.45 μm because some larger colloids are removed (Table 1).

Overall, our findings provide evidence that glaciers are important components of global Fe cycle. However, further estimates of truly dissolved Fe and colloidal/nanoparticulate Fe combined with sediment-bound Fe from glaciers are crucial for improving our understanding of the biogeochemical impacts of glacier discharge. Moreover, quantifying the magnitude and spatial-temporal dynamics of Fe, and their downstream behavior, will improve our insight into the role of glaciers in the global Fe cycle in a warming climate.

5. Conclusions

Concentrations of filtered iron (dFe; <0.45 μm) from three glaciers in Asia were continuously monitored over an entire melt season. Seasonal mean dFe concentrations ranged from 818 to 1,559 nM at DG, UG1, and LHG, and there were increasing downstream dFe concentrations at DG. Concentrations of dFe exhibited strong seasonality (222–4,298 nM), with higher values in low-flow shoulder seasons and lower values during peak flows in midsummer. We found that the ratios of monthly to seasonal dFe concentrations during June to September (ranging 0.63 to 1.85) can be used to estimate seasonal mean dFe concentrations sampled during limited melt seasons, and the power law relationship between daily dFe concentrations and glacier discharge can be used to estimate the seasonal exports of dFe from adjacent glaciers where only discharge is available. Utilizing current data, combined with previously published data, we produced an estimate of dFe release from ASG (23.8 Gg/a). dFe from ASG plus other five regions (ALG, CEG, SJG, LLG, and ICG) indicates a global dFe flux of 185 Gg/a, which is 3.6 to 9.5 times higher than the export from ice sheets. dFe yields from glaciers followed a power law of the form yields=50 (specific discharge)$^{1.28}$ that was first identified by Hodson et al. (2017). Our findings indicate that glaciers provide a substantial source of potentially labile Fe and may become increasingly important for global Fe biogeochemical cycles. Future studies should be conducted on long-term biogeochemical evolution at glacial basins with different proglacial environments, bedrock composition, and weathering intensity, which is crucial for improving our understanding of the ecological impacts of glaciers against global warming.

Acknowledgments
We sincerely thank R. Xu, D.,Y. Hui, and S.,P. Gao for laboratory analysis; W. Q. Guo for helping to draw Figure 1; J. K. Wu and W. J. Sun for sharing field data; and two anonymous reviewers, whose thoughtful comments significantly improved this manuscript. This work was funded by the National Natural Science Foundation of China (41671053 and 91647102), the Fundamental Research Funds for the Central Universities (2018B10214), the National Natural Science Foundation of China (41730751, 41771040, 41671071, and 41771084), the Open Foundation of State Key Laboratory of Cryospheric Sciences (SKLCS-OP-2019-04), the Open Foundation of State Key Laboratory of Frozen Soil Engineering (SKLFSE201411), the Special Fund of State Key Laboratory of Hydrology-Water Resources and Hydraulic Engineering (20145027312), Academy of Finland (268170), the Independent Program of the State Key Laboratory of Cryospheric Sciences (SKLCS-ZZ-2019), and the Alaska Climate Adaptation Science Center. The authors declare no conflicts of interest. All data used in this study have been submitted to the National Snow and Ice Data Center and are freely available for download (https://nsidc.org/node/4569/submission/31084).

References

Aciego, S. M., Stevenson, E. I., & Arendt, C. A. (2015). Climate versus geological controls on glacial meltwater micronutrient production in southern Greenland. *Earth and Planetary Science Letters*, *424*, 51–58. https://doi.org/10.1016/j.epsl.2015.05.017

Bamber, J., van den Broeke, M., Ettema, J., Lenaerts, J., & Rignot, E. (2012). Recent large increases in freshwater fluxes from Greenland into the North Atlantic. *Geophysical Research Letters*, *39*, L19501. https://doi.org/10.1029/2012GL052552

Bhatia, M. P., Kujawinski, E. B., Das, S. B., Breier, C. F., Henderson, P. B., & Charette, M. A. (2013). Greenland meltwater as a significant and potentially bioavailable source of iron to the ocean. *Nature Geoscience*, *6*, 274–278.

Bliss, A., Hock, R., & Radić, V. (2014). Global response of glacier runoff to twenty-first century climate change. *Journal of Geophysical Research: Earth Surface*, *119*, 717–730. https://doi.org/10.1002/2013JF002931

Brown, G. H. (2002). Glacier meltwater hydrochemistry. *Applied Geochemistry*, *17*(7), 855–883. https://doi.org/10.1016/S0883-2927(01)00123-8

Brown, G. H., Sharp, M., & Tranter, M. (1996). Experimental investigations of the weathering of suspended sediment by Alpine glacial meltwater. *Hydrological Processes*, *10*(4), 579–597. https://doi.org/10.1002/(SICI)1099-1085(199604)10:4<579::AID-HYP393>3.0.CO;2-D

Brown, G. H., Sharp, M., Tranter, M., Gurnell, A. M., & Nienow, P. W. (1994). Impact of post-mixing chemical reactions on the major ion chemistry of bulk meltwaters draining the Haut Glacier d'Arolla, Valais, Switzerland. *Hydrological Processes*, *8*(5), 465–480. https://doi.org/10.1002/hyp.3360080509

De Baar, H. J. W., & de Jong, J. T. M. (2001). Distribution, sources and sinks of iron in seawater. In D. R. Turner, & K. A. Hunter (Eds.), *The Biogeochemistry of Iron in Seawater*, (pp. 123–253). New York: Wiley.

Dieng, H. B., Cazenave, A., Meyssignac, B., & Ablain, M. (2017). New estimate of the current rate of sea level rise from a sea level budget approach. *Geophysical Research Letters*, *44*, 3744–3751. https://doi.org/10.1002/2017GL073308

Dong, Z., Qin, D., Chen, J., Qin, X., Ren, J., Cui, X., et al. (2014). Physicochemical impacts of dust particles on alpine glacier meltwater at the Laohugou Glacier basin in western Qilian Mountains, China. *Science of the Total Environment*, *493*, 930–942. https://doi.org/10.1016/j.scitotenv.2014.06.025

Fortner, S. K., Mark, B. G., McKenzie, J. M., Bury, J., Trierweiler, A., Baraer, M., et al. (2011). Elevated stream trace and minor element concentrations in the foreland of receding tropical glaciers. *Applied Geochemistry*, *26*(11), 1792–1801. https://doi.org/10.1016/j.apgeochem.2011.06.003

Fretwell, P. T., Pritchard, H. D., Vaughan, D. G., Bamber, J. L., Barrand, N. E., Bell, R., et al. (2013). Bedmap2: Improved ice bed, surface and thickness datasets for Antarctica. *The Cryosphere*, *7*(1), 375–393. https://doi.org/10.5194/tc-7-375-2013

Galeczka, I., Oelkers, E. H., & Gislason, S. R. (2014). The chemistry and element fluxes of the July 2011 Múlakvísl and Kaldakvísl glacial floods, Iceland. *Journal of Volcanology and Geothermal Research*, *273*, 41–57. https://doi.org/10.1016/j.jvolgeores.2013.12.004

Green, W. J., Stage, B. R., Preston, A., Wagers, S., Shacat, J., & Newell, S. (2005). Geochemical processes in the Onyx River, Wright Valley, Antarctica: major ions, nutrients, trace metals. *Geochimica et Cosmochimica Acta*, *69*(4), 839–850. https://doi.org/10.1016/j.gca.2004.08.001

Hallet, B., Hunter, L., & Bogen, J. (1996). Rates of erosion and sediment evacuation by glaciers: A review of field data and their implications. *Global and Planetary Change*, *12*(1-4), 213–235. https://doi.org/10.1016/0921-8181(95)00021-6

Han, T., Li, X., Gao, M., Mika, Sillanpää, Pu, H., & Lu, C. (2015). Electrical conductivity during the ablation process of the Glacier No.1 at the headwater of the Urumqi River in the Tianshan Mountains. *Arctic, Antarctic, and Alpine Research*, *47*(2), 327–334. https://doi.org/10.1657/AAAR00C-13-138

Han, T., Pu, H., Cheng, P., & Jiao, K. (2016). Hydrological effects of alpine permafrost in the head of Urumqi River, Tianshan Mountains. *Sciences in Cold and Arid Regions*, *8*, 241–249.

Hawkings, J. R., Wadham, J. L., Tranter, M., Raiswell, R., Benning, L. G., Statham, P. J., et al. (2014). Ice sheets as a significant source of highly reactive nanoparticulate iron to the oceans. *Nature Communications*, *5*(1), 3929. https://doi.org/10.1038/ncomms4929

Hodgkins, R. (2001). Seasonal evolution of meltwater generation, storage and discharge at a non-temperate glacier in Svalbard. *Hydrological Processes*, *15*, 441–460.

Hodgkins, R., Cooper, R., Tranter, M., & Wadham, J. L. (2013). Drainage-system development in consecutive melt seasons at a polythermal, Arctic glacier, evaluated by flow-recession analysis and linear-reservoir simulation. *Water Resources Research*, *49*, 4230–4243. https://doi.org/10.1002/wrcr.20257

Hodgkins, R., Tranter, M., & Dowdeswell, J. A. (1997). Solute provenance, transport and denudation in a High-Arctic glacierised basin. *Hydrological Processes*, *11*(14), 1813–1832. https://doi.org/10.1002/(SICI)1099-1085(199711)11:14<1813::AID-HYP498>3.0.CO;2-C

Hodson, A., Heaton, T., Langford, H., & Newsham, K. (2010). Chemical weathering and solute export by meltwater in a maritime Antarctic glacier basin. *Biogeochemistry*, *98*, 9–27.

Hodson, A., Nowak, A., & Christiansen, H. (2016). Glacial and periglacial floodplain sediments regulate hydrologic transfer of reactive iron to a high arctic fjord. *Hydrological Processes*, *30*(8), 1219–1229. https://doi.org/10.1002/hyp.10701

Hodson, A., Nowak, A., Sabacka, M., Jungblut, A., Navarro, F., Pearce, D., et al. (2017). Climatically sensitive transfer of iron to maritime Antarctic ecosystems by surface runoff. *Nature Communications*, *8*(1), 14,499. https://doi.org/10.1038/ncomms14499

Hodson, A., Porter, P., Lowe, A., & Mumford, P. (2002). Chemical denudation and silicate weathering in Himalayan glacier basins: Batura Glacier, Pakistan. *Journal of Hydrology*, *262*(1-4), 193–208. https://doi.org/10.1016/S0022-1694(02)00036-7

Hodson, A., Tranter, M., & Vatne, G. (2000). Contemporary rates of chemical denudation and atmospheric CO_2 sequestration in glacier basins: An Arctic perspective. *Earth Surface Processes and Landforms*, *25*(13), 1447–1471. https://doi.org/10.1002/1096-9837(200012)25:13<1447::AID-ESP156>3.0.CO;2-9

Hood, E., Battin, T. J., Fellman, J., O'Neel, S., & Spencer, R. G. M. (2015). Storage and release of organic carbon from glaciers and ice sheets. *Nature Geoscience*, *8*(2), 91–96. https://doi.org/10.1038/ngeo2331

Hubbard, B., & Nienow, P. (1997). Alpine subglacial hydrology. *Quaternary Science Reviews*, *16*(9), 939–955. https://doi.org/10.1016/S0277-3791(97)00031-0

Hubbard, B. P., Sharp, M., Willis, I. C., Nielsen, M. K., & Smart, C. C. (1995). Borehole water-level variations and the structure of the subglacial hydrological system of Haut Glacier d'Arolla, Valais, Switzerland. *Journal of Glaciology*, *41*(139), 572–583. https://doi.org/10.1017/S0022143000034894

IPCC Climate Change (2013). In T. F. Stocker, et al. (Eds.), *The Physical Science Basis*. Cambridge: Cambridge Univ. Press.

Kargel, J. S., Ahlstrøm, A. P., Alley, R. B., Bamber, J. L., Benham, T. J., Box, J. E., et al. (2012). Greenland's shrinking ice cover: "Fast times" but not that fast. *The Cryosphere*, *6*(3), 533–537. https://doi.org/10.5194/tc-6-533-2012

Kısakurek, B., James, R. H., & Harris, N. B. W. (2005). Li and δ^7Li in Himalayan rivers: proxies for silicate weathering? *Earth and Planetary Science Letters*, *237*(3-4), 387–401. https://doi.org/10.1016/j.epsl.2005.07.019

Li, X. (2009). Hydrochemical characteristics of meltwater from glaciers at the typical catchments in western China. The doctoral thesis, Chinese Academy of Sciences.

Li, X., Ding, Y., Han, T., Kang, S., Yu, Z., & Jing, Z. (2019). Seasonal controls of runoff chemistry and chemical weathering at Urumqi Glacier No.1 basin in central Asia. *Hydrological Processes*. https://doi.org/10.1002/hyp.13555

Li, X., Ding, Y., Xu, J., He, X., Han, T., Kang, S., et al. (2018). Importance of mountain glaciers as a source of dissolved organic carbon. *Journal of Geophysical Research: Earth Surface*, *123*, 2123–2134. https://doi.org/10.1029/2017JF004333

Li, X., He, X., Kang, S., Mika, Sillanpää, Ding, Y., Han, T., et al. (2016). Diurnal dynamics of minor and trace elements in stream water draining Dongkemadi Glacier on the Tibetan Plateau and its environmental implications. *Journal of Hydrology*, *541*, 1104–1118. https://doi.org/10.1016/j.jhydrol.2016.08.021

Li, X., Qin, D., Jing, Z., Li, Y., & Wang, N. (2013). Diurnal hydrological controls and non-filtration edFects on minor and trace elements in stream water draining the Qiyi Glacier, Qilian Mountain. *Science China Earth Sciences*, *56*(1), 81–92. https://doi.org/10.1007/s11430-012-4480-6

Lippiatt, S. M., Lohan, M. C., & Bruland, K. W. (2010). The distribution of reactive iron in northern Gulf of Alaska coastal waters. *Marine Chemistry*, *121*(1-4), 187–199. https://doi.org/10.1016/j.marchem.2010.04.007

Liu, L., Ren, J., & Qin, D. (2000). Chemical characteristics at the head of Rongbuk River on Mt. Everest. *Environmental Sciences*, *21*, 59–63.

Liu, S., Yao, X., Guo, W., Xu, J., Shangguan, D., Wei, J., et al. (2015). The contemporary glaciers in China based on the Second Chinese Glacier Inventory. *Acta Geographica Sinica*, *70*, 3–16.

Lutz, A. F., Immerzeel, W. W., Shrestha, A. B., & Bierkens, M. F. P. (2014). Consistent increase in High Asia's runoff due to increasing glacier melt and precipitation. *Nature Climate Change*, *4*(7), 587–592. https://doi.org/10.1038/nclimate2237

Lyons, W. B., Dailey, K. R., Welch, K. A., Deuerling, K. M., Welch, S. A., & McKnight, D. M. (2015). Antarctic streams as a potential source of iron for the Southern Ocean. *Geology*, *43*(11), 1003–1006. https://doi.org/10.1130/G36989.1

Martin, J. H., Fitzwater, S. E., & Gordon, R. M. (1990). Iron deficiency limits phytoplankton growth in Antarctic waters. *Global Biogeochemical Cycles*, *4*(1), 5–12. https://doi.org/10.1029/GB004i001p00005

Meier, M. F., Dyurgerov, M. B., Rick, U. K., O'Neel, S., PfedFer, W. T., Anderson, R. S., et al. (2007). Glaciers dominate eustatic sea-level rise in 21st century. *Science*, *317*(5841), 1064–1067. https://doi.org/10.1126/science.1143906

Mitchell, A. C., & Brown, G. H. (2007). Diurnal hydrological-physicochemical controls and sampling methods for minor and trace elements in an Alpine glacial hydrological system. *Journal of Hydrology*, *332*(1-2), 123–143. https://doi.org/10.1016/j.jhydrol.2006.06.026

Mitchell, A. C., Brown, G. H., & Fuge, R. (2001). Minor and trace element export from a glacierized Alpine headwater catchment (Haut Glacier d'Arolla, Switzerland). *Hydrological Processes*, *15*(18), 3499–3524. https://doi.org/10.1002/hyp.1041

Nielsdottir, M. C., Moore, C. M., Sanders, R., Hinz, D. J., & Achterberg, E. P. (2009). Iron limitation of the postbloom phytoplankton communities in the Iceland Basin. *Global Biogeochemical Cycles*, *23*, GB3001. https://doi.org/10.1029/2008GB003410

Nienow, P., Sharp, M., & Willis, I. (1998). Seasonal changes in the morphology of the subglacial drainage system, Haut Glacier D'Arolla, Switzerland. *Earth Surface Processes and Landforms*, *23*(9), 825–843. https://doi.org/10.1002/(SICI)1096-9837(199809)23:9<825::AID-ESP893>3.0.CO;2-2

Nowak, A., & Hodson, A. (2015). On the biogeochemical response of a glacierized High Arctic watershed to climate change: revealing patterns, processes and heterogeneity among micro-catchments. *Hydrological Processes*, *29*(6), 1588–1603. https://doi.org/10.1002/hyp.10263

Pfeffer, W. T., Arendt, A. A., Bliss, A., Bolch, T., Cogley, J. G., Gardner, A. S., et al. (2014). The Randolph Glacier Inventory: A globally complete inventory of glaciers. *Journal of Glaciology*, *60*(221), 537–552. https://doi.org/10.3189/2014JoG13J176

Radić, V., Bliss, A., Beedlow, A. C., Hock, R., Miles, E., & Cogley, J. G. (2014). Regional and global projections of twenty-first century glacier mass changes in response to climate scenarios from global climate models. *Climate Dynamics*, *42*(1-2), 37–58. https://doi.org/10.1007/s00382-013-1719-7

Raiswell, R. (2011). Iceberg-hosted nanoparticulate Fe in the Southern Ocean: Mineralogy, origin, dissolution kinetics and source of bioavailable Fe. *Deep Sea Research, Part II*, *58*(11-12), 1364–1375. https://doi.org/10.1016/j.dsr2.2010.11.011

Raiswell, R., & Canfield, D. E. (2012). The iron biogeochemical cycle past and present. *Geochemical Perspectives*, *1*(1), 1–220. https://doi.org/10.7185/geochempersp.1.1

Raiswell, R., Hawkings, J. R., Elsenousy, A., Death, R., Tranter, M., & Wadham, J. L. (2018). Iron in glacial systems: Speciation, reactivity, freezing behavior and alteration during transport. *Frontiers in Earth Science*, *6*, 222. https://doi.org/10.3389/feart.2018.00222

Raiswell, R., Hawkings, J. R., Benning, L. G., Baker, A. R., Death, R., Albani, S., et al. (2016). Potentially bioavailable iron delivery by iceberg-hosted sediments and atmospheric dust to the polar oceans. *Biogeosciences*, *13*(13), 3887–3900. https://doi.org/10.5194/bg-13-3887-2016

Rignot, E., Bamber, J. L., van den Broeke, M. R., Davis, C., Li, Y., Jan Van De Berg, W., & van Meijgaard, E. (2008). Recent Antarctic ice mass oss from radar interferometry and regional climate modelling. *Nature Geoscience*, *1*(2), 106–110. https://doi.org/10.1038/ngeo102

Schroth, A. W., Crusius, J., Chever, F., Bostick, B. C., & Rouxel, O. J. (2011). Glacial influence on the geochemistry of riverine iron fluxes to the Gulf of Alaska and edFects of deglaciation. *Geophysical Research Letters*, *38*, L16605. https://doi.org/10.1029/2011GL048367

Schroth, A. W., Crusius, J., Hoyer, I., & Campbell, R. (2014). Estuarine removal of glacial iron and implications for iron fluxes to the ocean. *Geophysical Research Letters*, *41*, 3951–3958. https://doi.org/10.1002/2014GL060199

Sharp, M., Tranter, M., Brown, G. H., & Skidmore, M. (1995). Rates of chemical denudation and CO_2 drawdown in a glacier-covered alpine basin. *Geology*, *23*(1), 61–64. https://doi.org/10.1130/0091-7613(1995)023<0061:ROCDAC>2.3.CO;2

Song, G., Wang, N., Chen, L., He, J., Jiang, X., & Wu, X. (2008). Analysis of the recent features of the meltwater runoff from the Qiyi Glacier, Qilian Mountains. *Journal of Glaciology and Geocryology*, *30*, 321–328.

Statham, P. J., Skidmore, M., & Tranter, M. (2008). Inputs of glacially derived dissolved and colloidal iron to the coastal ocean and implications for primary productivity. *Global Biogeochemical Cycles*, *22*, GB3013. https://doi.org/10.1029/2007GB003106

Tranter, M., Brown, G. H., Raiswell, R., Sharp, M., & Gurnell, A. (1993). A conceptual model of solute acquisition by Alpine glacial meltwaters. *Journal of Glaciology*, *39*(133), 573–581. https://doi.org/10.1017/S0022143000016464

Wadham, J. L., Hodgkins, R., Cooper, R. J., & Tranter, M. (2001). Evidence for seasonal subglacial outburst events at a polythermal glacier, Finsterwalderbreen, Svalbard. *Hydrological Processes*, *15*(12), 2259–2280. https://doi.org/10.1002/hyp.178

Wang, J., Xu, J., Zhang, S., Liu, S., & Han, H. (2010). Chemical Denudation Rates and Carbon Dioxide Sink in Koxkar Glacierised Region at the South Slope of Mt. Tianshan, China. *Environmental Sciences*, *31*, 903–910.

Wu, W., Xu, S., Yang, J., Yin, H., & Tao, X. (2009). Sr fluxes and isotopic compositions in the headwaters of the YA, Tongtian River and Jinsha River originating from the Qinghai-Tibet Plateau. *Chemical Geology*, *260*(1-2), 63–72. https://doi.org/10.1016/j.chemgeo.2008.12.007

Yde, J. C., Knudsen, N. T., Hasholt, B., & Mikkelsen, A. B. (2014). Meltwater chemistry and solute export from a Greenland Ice Sheet catchment, Watson River, West Greenland. *Journal of Hydrology*, *519*, 2165–2179. https://doi.org/10.1016/j.jhydrol.2014.10.018

Yde, J. C., Knudsen, N. T., & Nielsen, O. B. (2005). Glacier hydrochemistry, solute provenance, and chemical denudation at a surge-type glacier in Kuannersuit Kuussuat, Disko Island, West Greenland. *Journal of Hydrology*, *300*(1-4), 172–187. https://doi.org/10.1016/j.jhydrol.2004.06.008

Yde, J. C., Riger-Kusk, M., Christiansen, H. H., Knudsen, N. T., & Humlum, O. (2008). Hydrochemical characteristics of bulk meltwater from an entire ablation season, Longyearbreen, Svalbard. *Journal of Glaciology*, *54*(185), 259–272. https://doi.org/10.3189/002214308784886234

Zhang, R., John, S. G., Zhang, J., Ren, J., Wu, Y., Zhu, Z., et al. (2015). Transport and reaction of iron and iron stable isotopes in glacial meltwaters on Svalbard near Kongsfjorden: From rivers to estuary to ocean. *Earth and Planetary Science Letters*, *424*, 201–211. https://doi.org/10.1016/j.epsl.2015.05.031